

Measurement of the spin-orbit Zeeman magnetic field in a two-dimensional electron system with a small zero-field spin splitting

R. G. Mani,^{*†} J. H. Smet,[†] K. von Klitzing,[†] V. Narayanamurti,^{*‡} W. B. Johnson,[§] and V. Umansky[¶]

^{*}Harvard University, Gordon McKay Laboratory of Applied Science, 9 Oxford Street, Cambridge, MA 02138, USA

[†]Max-Planck-Institut für Festkörperforschung, Heisenbergstrasse 1, 70569 Stuttgart, Germany

[‡]Harvard University, 217 Pierce Hall, 29 Oxford Street, Cambridge, MA 02138, USA

[§]Laboratory for Physical Sciences, University of Maryland, College Park, MD 20740, USA

[¶]Braun Center for Submicron Research, Weizmann Institute, Rehovot 76100, Israel

(Submitted: March 3, 2003)

Abstract

We suggest an approach for characterizing the spin-orbit interaction in high mobility 2D electron systems described by a small zero-field spin splitting, in specimens where beats are not readily observable in the Shubnikov-de Haas effect. The Zeeman magnetic field seen in the reference frame of the electron is evaluated from a quantitative study of beats observed in radiation-induced magnetoresistance oscillations.

The charge degree of freedom of the electron has made possible the information technology revolution through devices such as the transistor, the integrated circuit, the light emitting diode, and the diode laser.¹ Recently, research has focused upon the utilization of the supplementary spin degree of freedom of the electron,²⁻⁴ and initial successes based on this approach, such as spin sensitive magnetic sensors based on magnetic multilayers,⁴ and non-volatile magnetic memory,^{2,3} have greatly stimulated the "spintronics" paradigm, which aspires to realize desired device characteristics such as low power utilization, high speed, and persistence of memory even in the absence of power.^{2,4}

The application and control of the magnetic field seen in the reference frame of the electron due to the spin-orbit interaction is a spintronics theme that is embodied in the spin transistor.⁵⁻⁸ This transistor modulates the device-current by regulating the spin-precession of electrons over a gate-controlled two-dimensional electron channel, between ferromagnetic (spin-polarizing) source and (spin-analyzing) drain contacts.⁸ As the effective magnetic field seen by electrons in this device develops from the normal electric field at the heterojunction interface ("Rashba effect"),⁷ this magnetic field can, in principle, be controlled by an electrical gate.⁸ The so-called Rashba term, proportional to the electron wavevector k , is believed to account for most of the observed Zero-field Spin Splitting (ZFSS) in the narrow gap InGaAs/InAlAs two-dimensional electron system (2DES).⁸ In the 2DES realized in the intermediate gap GaAs/AlGaAs system, a Bulk Inversion Asymmetry (BIA) contribution to the ZFSS, provides another magnetic field contribution in the reference frame of the electron.⁹⁻¹¹ Although theory has suggested that the BIA term is stronger than the Rashba term in the 2DES realized on GaAs/AlGaAs heterostructures,¹¹ ZFSS in n-type GaAs/AlGaAs is not so easily characterized by experiment

because associated physical effects are often difficult to detect using available methods.

Typical transport investigations of the 2DES study the ZFSS by looking for beats in the Shubnikov-de Haas (SdH) oscillations originating from the dissimilar Fermi surfaces for the spin-split bands.¹²⁻¹⁴ However, the effectiveness of this approach depends upon both the observability of SdH oscillations, and the occurrence of a sufficiently large spin splitting, such that a beat becomes discernible well above the lowest magnetic field at which SdH oscillations occur in the specimen. In GaAs/AlGaAs heterostructures with 2 dimensional electrons, these conditions are not easily realized and therefore beats in SdH oscillations due to a ZFSS are often unobservable, even in the highest mobility material. In addition, it is not easy to unambiguously relate the observation of SdH beats with ZFSS because other mechanisms, such as sample inhomogeneity and magneto-intersubband scattering, can, in principle, provide similar experimental signatures.¹³⁻¹⁵ Thus, a need exists for additional experimental techniques for investigating the spin-orbit interaction in the 2DES characterized by a small spin splitting, to supplement the SdH, Raman scattering, and Electron Spin Resonance based approaches.^{13,16,17} Here, we propose a sensitive method for determining the ZFSS in the GaAs/AlGaAs 2DES, in specimens where beats may not be discernible in the SdH effect. This technique might be applied to track changes in the spin-orbit interaction in the GaAs/AlGaAs 2DES that result from the controlled modification of the device structure, and this could prove helpful for the development of spintronics based on this system.^{2,3}

Experiments were carried out on Hall bars and square shaped devices fabricated from GaAs/AlGaAs heterostructures grown by Molecular-Beam-Epitaxy (MBE). Upon slow cooling in the dark, the realized 2DES was typically characterized by a low electron density n (4.2 K) \approx

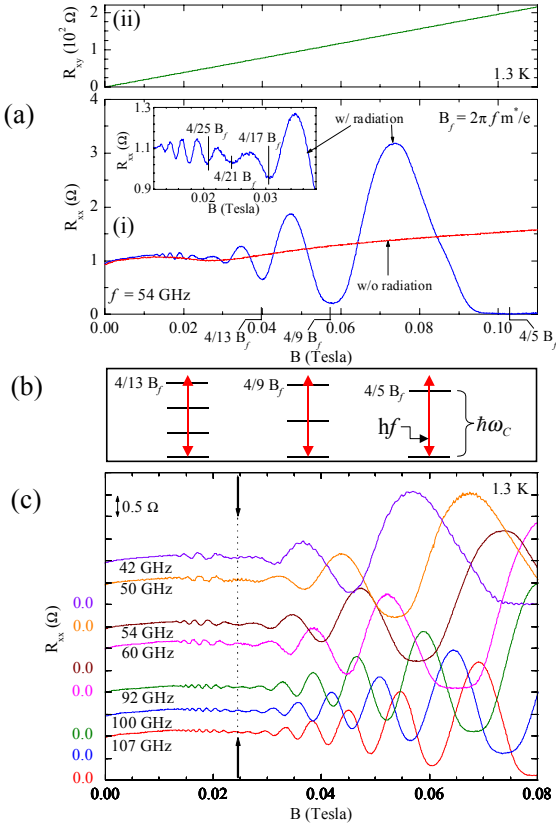


Fig. 1) (a) (i): The resistance R_{xx} over low magnetic fields in a GaAs/AlGaAs heterostructure with (w/) and without (w/o) electromagnetic wave excitation at 54 GHz. (ii): The Hall resistance (R_{xy}) w/o radiation. The R_{xx} minima occur about $B = [4/(4j+1)] B_f$, and these field values are marked for the first few minima in (i). The beat, which is observable in the oscillatory resistance, is expanded in the inset of (i). Note that the minima continue to follow the empirical rule through the beat.

(b) This panel illustrates the incommensurability between the photon energy, hf , and integral cyclotron energies, $j\hbar\omega_C$, in the vicinity of the resistance minima, i.e., $hf = ([4j+1]/4)\hbar\omega_C$ at $B = (4/[4j+1]) B_f$ with $j = 1,2,3\dots$

(c) The radiation induced magnetoresistance oscillations are shown for a set of electromagnetic wave frequencies. Here the beat remains fixed in the vicinity of $B = 0.024$ Tesla as the resistance-oscillation frequency changes with the radiation frequency.

$1.5 \times 10^{11} \text{ cm}^{-2}$ condition. Subsequent brief illumination by a red LED produced $n(4.2 \text{ K}) \equiv 3 \times 10^{11} \text{ cm}^{-2}$ and an electron mobility $\mu(1.5 \text{ K}) \equiv 1.5 \times 10^7 \text{ cm}^2/\text{Vs}$. Low frequency lock-in based four-terminal measurements of the resistance and the Hall effect were carried out with the sample mounted inside a waveguide and immersed in pumped liquid Helium, for temperatures, T , in the range $1.3 \leq T \leq 4.2 \text{ K}$. Electromagnetic waves in the microwave part of the spectrum, $27 \leq f \leq 120 \text{ GHz}$, were generated using tunable sources that covered, piecewise, the above mentioned f -range. The EM wave power level was set at the source and then reduced using variable attenuators. The power level in the vicinity of the sample is estimated to be less than 1 mW.

Fig. 1(a) illustrates the magnetoresistance observed with (w/) and without (w/o) microwave excitation, in the high mobility condition. Without radiation, weak magnetoresistance is characterized by the absence of the SdH effect to $B = 0.11$ Tesla at $T = 1.3 \text{ K}$ (see Fig. 1(a)(i)). Excitation of the specimen with electromagnetic waves induces oscillations in the resistance and a remarkable zero-resistance-state over a broad B -interval in the vicinity of 0.1 Tesla.¹⁸⁻²¹ Fig. 1 (a)(i) shows that the three deepest resistance minima occur about $4/5 B_f$, $4/9 B_f$, and $4/13 B_f$, where $B_f = 2\pi f m^*/e$, $m^* = 0.067 \text{ m}$ is the electron effective mass, and e is the electric charge. Such resistance minima generally form about $B = (4/4j+1) B_f$, with $j=1,2,3\dots$, where there is a mismatch between the photon energy, hf , and an integer number, j , of cyclotron energies, $j\hbar\omega_C$, as illustrated in Fig 1(b).¹⁸⁻¹⁹ The reader is directed elsewhere for related theory.¹⁹⁻²³

The subject here is the non-monotonic variation in the amplitude of the resistance oscillations, which leads to a 'beat,' as the oscillations become weaker, when one moves to progressively lower B (see Fig. 1(a)(i) and Fig. 1(a)(i), inset). This effect also occurs in the data presented in ref. 21. A noteworthy point, see Fig. 1(a)(i), is that there does not appear to be a 180° phase change in the resistance oscillations as one moves through the beat, i.e., the resistance minima continue to occur at magnetic fields given by $B = [4/(4j+1)] B_f$. In Fig. 1(c), resistance data are shown for a number of microwave frequencies. These data show that the beat in the oscillatory resistance remains at a constant B , $B \equiv 0.024$ Tesla, with the change in f .

A lineshape study was carried out in order to further characterize these oscillations and help to understand the origin of the beats. Initial studies¹⁸ suggested that the oscillations could be fit over a narrow B -window with an exponentially damped sinusoid: $R_{xx}^{\text{osc}} = A' \exp(-\lambda/B) \sin(2\pi F/B - \pi)$, where A' is the amplitude, λ is the damping factor, and F is the fundamental field for the resistance oscillations. In order to account for the beat, a simple candidate lineshape that included superposition of two such waveforms: $R_{xx}^{\text{osc}} = A' \exp(-\lambda/B) [\sin(2\pi F_1/B - \pi) + \sin(2\pi F_2/B - \pi)] = A \exp(-\lambda/B) \sin(2\pi F/B - \pi) \cos(2\pi \Delta F/B)$ where $F = (F_1+F_2)/2$ and $\Delta F = (F_1-F_2)/2$, was initially applied to the data. Least squares fits with this lineshape proved unsatisfactory in reproducing the data because this lineshape exhibits a phase reversal in the magnetoresistance oscillations through a beat, unlike experiment, see Fig. 1(a)(i). Thus, line-fit studies were also carried out with the waveform $R_{xx}^{\text{osc}} = A \exp(-\lambda/B) \sin(2\pi F/B - \pi) [1 + \cos(2\pi \Delta F/B)]$, which exhibits beats without phase reversal.

Fig. 2 illustrates data obtained at a fixed f as a function of the power level for three power attenuation factors. Also shown in the figure is a fit to the data, using the lineshape $R_{xx}^{\text{osc}} = A \exp(-\lambda/B) \sin(2\pi F/B - \pi) [1 + \cos(2\pi \Delta F/B)]$. Inspection shows a good agreement between data and fit over the fitting interval. A comparison of Fig. 2 (a), (b), and

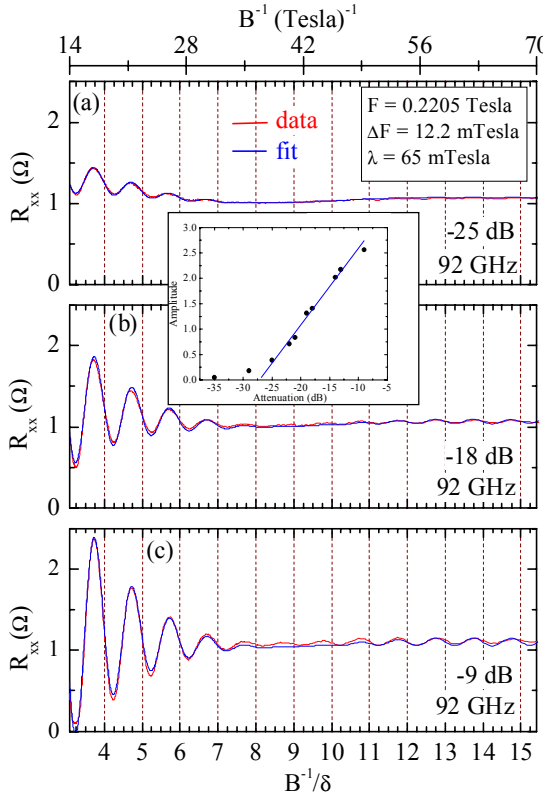


Fig. 2) Magnetoresistance oscillations are exhibited for three power levels in panels (a) - (c) vs. B^{-1} (top axis) and B^{-1}/δ (bottom axis). Here, δ is the period in B^{-1} , i.e., $\delta = F^{-1}$, where F has been determined by fitting the data to the empirical lineshape $R_{xx}^{osc} = A \exp(-\lambda/B) \sin(2\pi F/B - \pi) [1 + \cos(2\pi\Delta F/B)]$. The resistance minima occur about $B^{-1}/\delta = (4/[4j+1])^{-1}$ over the entire range.

(Inset): The amplitude, A , of the resistance oscillations, which has been determined from the fit to empirical lineshape, is plotted vs. the power attenuation factor in decibels (dB).

(c) shows a monotonic increase in the amplitude of the oscillations with increasing the microwave power level, that is reproduced by the fit parameter, A , see Fig. 2, inset. The other fit parameters F , ΔF , and λ , shown in the inset to Fig. 2(a), were held constant in data fits vs. the power attenuation factor. The oscillation period, δ , where $\delta = 1/F$, has been used to renormalize the inverse field axis, as in the lower abscissa of Fig. 2. The plot of the data in terms of this dimensionless variable shows that one set of nodes in the oscillations occur at $B^{-1}/\delta = F/B = j$, where $j = 1, 2, 3, \dots$, while resistance minima transpire about $B^{-1}/\delta = [4/(4j+1)]^{-1}$.

Representative data and fit at a pair of f , exhibited in Fig 3. (a) and (b), show that this lineshape also describes the data obtained at widely spaced f . Indeed, this lineshape provided a good description of the oscillatory magnetoresistance over the examined frequency range. A summary of the fit parameters, F , ΔF , and λ , is presented in Fig. 4. The noteworthy features in the f - dependence of the fit parameters are: (i) F or, equivalently, the fundamental

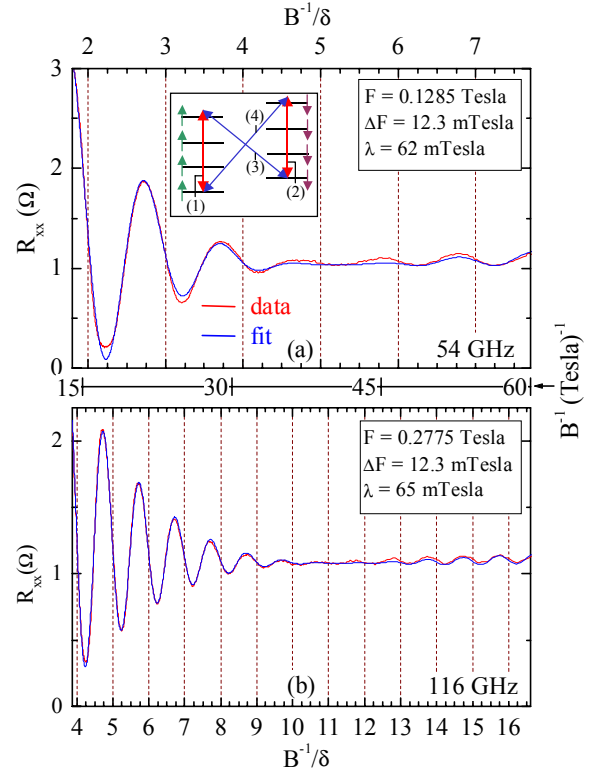


Fig. 3) The figure shows the radiation induced magnetoresistance oscillations at (a) 54 GHz and (b) 116 GHz, along with a fit of the data with the expression $R_{xx}^{osc} = A \exp(-\lambda/B) \sin(2\pi F/B - \pi) [1 + \cos(2\pi\Delta F/B)]$. The bottom- and top- axis show B^{-1}/δ , where $\delta = F^{-1}$, and F is the resistance oscillation frequency obtained from the lineshape fit. The center abscissa shows the inverse magnetic field.

Inset to (a): The lineshape utilized in the data-fit may be attributed to four types of radiation-induced transitions in the vicinity of the Fermi surface, as cartooned here. Here, the spin-up and spin-down Landau levels are shown shifted with respect to each other due to a finite splitting as $B \rightarrow 0$, due to the spin-orbit interaction. Transitions of type 1 and 2 are spin-preserving transitions, while transitions of type 3 and 4 include spin-flip.

field for the resistance oscillations, increases linearly with f , (see Fig. 4(a)), and the increase is characterized by $dF/df = 2.39$ mTesla/GHz, consistent with $m^* = 0.067$ m.^{19,24} Further, $F = B_f$ within experimental uncertainty, which indicates that $F/B = hf/\hbar\omega_C$. (ii) The beat frequency, $\Delta F \approx 12.3$ mTesla, is independent of f (see Fig. 4(b)), consistent with Fig. 1(a)(i). And, (iii) the damping parameter λ , $\lambda \approx 65$ mTesla, is also approximately independent of f (see Fig. 4(c)).²⁵

The lineshape, $R_{xx}^{osc} = A \exp(-\lambda/B) \sin(2\pi F/B - \pi) [1 + \cos(2\pi\Delta F/B)]$, which has been used to describe the data, can be understood by invoking four distinct types of transitions between Landau subbands near the Fermi level, as qualitatively sketched in the inset of Fig. 3, with a series of magnetoresistance oscillations associated with each term. Here, the spin-orbit interaction helps to remove the spin degeneracy of Landau levels as $B \rightarrow 0$. Thus, the terms (1)

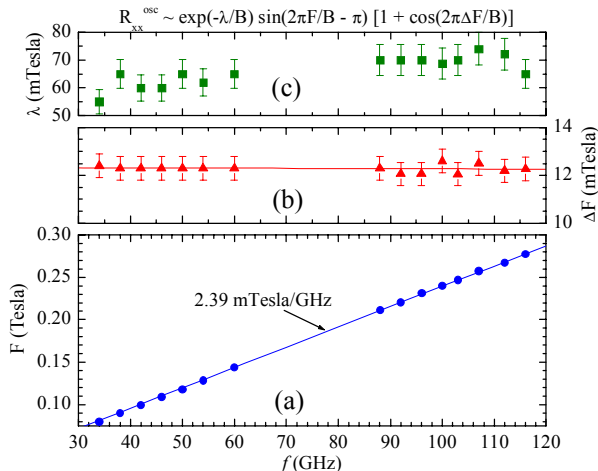


Fig. 4) A summary of the fit parameters obtained from the lineshape study of the radiation induced magnetoresistance oscillations in GaAs/AlGaAs heterostructures. (a) The resistance oscillation frequency, F , increases linearly with the radiation frequency and $dF/df = 2.39$ mTesla/GHz. (b) The beat frequency, ΔF , is independent of the radiation frequency, f , and $\Delta F \approx 12.3$ mTesla. (c) The damping parameter λ obtained from the lineshape fit appears to be independent, or weakly dependent, on the radiation frequency, f .

and (2) represent spin preserving inter Landau level transitions, and the terms (3) and (4) represent spin-flip transitions. If the resistance oscillations originating from these terms have equal amplitude and share the same damping parameter, then the observed resistance would exhibit a superposition of four terms: $R_{xx}^{osc} = A' \exp(-\lambda/B) [\sin(2\pi F/B - \pi) + \sin(2\pi F/B - \pi) + \sin(2\pi[F-\Delta F]/B - \pi) + \sin(2\pi[F+\Delta F]/B - \pi)] = A \exp(-\lambda/B) \sin(2\pi F/B - \pi) [1 + \cos(2\pi\Delta F/B)]$, which is the lineshape that has been used to fit the data.

Thus, beats observed in the radiation-induced resistance oscillations follow as a consequence of a zero-field spin splitting, due to the spin-orbit interaction.^{5-14,16,17} And, the beat frequency observed in the resistance oscillations, $\Delta F \sim 12.3$ mTesla, is a manifestation of the (Zeeman) magnetic field seen in the reference frame of the electron, in the absence of an externally applied magnetic field.¹¹ One might relate ΔF to the ZFSS by identifying the change, Δf , in the radiation frequency f that will produce a similar change in the resistance oscillation frequency F , i.e., $\Delta f = \Delta F/[dF/df]$, where ΔF is the beat frequency, and $dF/df = 2.39$ mTesla/GHz (see Fig. 4(a)). Then, the spin-splitting

determined from ΔF corresponds to $\Delta f = 5.15$ GHz or $E_S(B=0) = \hbar\Delta f = 21$ μ eV. From a study of the Electron Spin Resonance (ESR) at high magnetic fields, Stein et al.¹⁷ reported a zero-field spin splitting of 7.8 GHz for $n = 4.6 \times 10^{11}$ cm⁻², which complements this determination for $n \approx 3 \times 10^{11}$ cm⁻². Theory suggests that in the GaAs/AlGaAs heterostructure 2DES, both the bulk inversion asymmetry and the Rashba terms have similar magnitudes, while the BIA makes the stronger contribution by roughly a factor of four. De Andrade e Silva et al. have indicated that the upper bound for the total zero-field spin splitting is ≈ 80 μ eV.¹¹

Electron Spin Resonance (ESR) was also investigated in this material in order to trace the high-B spin splitting in our specimens. The ESR study showed that the spin resonance field, B^{ESR} , varies at the rate $dB^{ESR}/df = 0.184$ Tesla/GHz in the vicinity of filling factor $\nu = 1$, which implies that the effective Zeeman magnetic field experienced by electrons in this specimen is approximately $B^Z = [dB^{ESR}/df] \Delta f = 0.184$ GHz⁻¹ Tesla * 5.15 GHz = 0.95 Tesla. As the effective magnetic field due to the Rashba term is oriented perpendicular to both the direction of electron motion and the normal of the 2DES, while the field due to the BIA term lies along the direction of motion of the confined electrons, the B^Z reported here is associated with the magnitude of the vector obtained by adding these terms. Although this estimate for the $B \rightarrow 0$ Zeeman magnetic field appears, at first sight, to be rather large by laboratory standards, the small g-factor in GaAs/AlGaAs heterostructures implies a small spin splitting, $E_S = 21$ μ eV, for such a B^Z , especially in comparison to the Fermi energy (~ 10 meV). This implies that possible beats in the SdH oscillations would be expected at low B , well below the lowest magnetic field (~ 0.2 Tesla at 1.3 K) at which SdH oscillations were observed in this material.

In summary, magnetoresistance oscillations induced by electromagnetic wave excitation in GaAs/AlGaAs 2DES heterostructures exhibit beats, which remain at a constant magnetic field with changing radiation frequency. These beats have been attributed here to a small zero-field spin splitting originating from the spin-orbit interaction. It appears that such beats in radiation induced oscillations could be utilized to track changes in the spin-orbit interaction that result from the controlled modification of the semiconductor device structure, and this might prove helpful for the development of spintronic devices based on this system.²⁻⁴

1) S. Sze, *Physics of Semiconductor Devices* (John Wiley and Sons, New York, 1981).

2) G. A. Prinz, *Science* 282, 1660 (1998).

3) S. A. Wolf, D. D. Awschalom, R. A. Buhrman, M. J. Daughton, S. von Molnar, M. L. Roukes, A. Y. Chtchelkanova, D. M. Treger, *Science* 294, 1488 (2001).

4) M. N. Baibich, J. M. Broto, A. Fert, F. Nguyen Van Dau, P. Petroff, P. Etienne, G. Creuzet, A. Friederich, and J. Chazelas, *Phys. Rev. Lett.* 61, 2472 (1988).

5) G. Dresselhaus, *Phys. Rev.* 100, 580 (1955).

6) L. M. Roth, *Phys. Rev.* 173, 755 (1968).

7) Y. A. Bychkov and E. I. Rashba, *J. Phys. C.* 17, 6039 (1984).

8) S. Datta and B. Das, *Appl. Phys. Lett.* 56, 665 (1990).

9) G. Lommer, F. Malcher, and U. Rössler, *Phys. Rev. Lett.* 60, 728 (1988).

10) R. Eppenga and M. F. H. Schuurmans, *Phys. Rev. B.* 37, 10923 (1988).

11) E. A. De Andrade e Silva, G. C. La Rocca, and F. Bassani, *Phys. Rev. B* 50, 8523 (1994).

12) B. Das, D. C. Miller, S. Datta, R. Reifenberger, W. P. Hong, P. K. Bhattacharya, and M. Jaffe, *Phys. Rev. B* 39, 1411 (1989).

13) P. Ramvall, B. Kowalski, and P. Omling, *Phys. Rev. B* 55, 7160 (1997).

14) A. C. H. Rowe, J. Nehls, R. A. Stradling, and R. S. Ferguson, *Phys. Rev. B* 63, 201307 (2001).

15) T. H. Sander, S. N. Holmes, J. J. Harris, D. K. Maude, and J. C. Portal, *Phys. Rev. B* 58, 13856 (1998).

16) B. Jusserand, D. Richards, G. Allan, C. Priester, and B. Etienne, *Phys. Rev. B* 51, 4707 (1995).

17) D. Stein, K. von Klitzing, and G. Weimann, *Phys. Rev. Lett.* 51, 130 (1983).

18) R. G. Mani, J. H. Smet, K. von Klitzing, V. Narayanamurti, and V. Umansky, *Bull. Am. Phys. Soc.* 46, 972 (2001); R. G. Mani, J. H. Smet, K. von Klitzing, V. Narayanamurti, W. B. Johnson, and V. Umansky, in the Proceedings of the 26th International Conference on the Physics of Semiconductors, 29 July – 2 August 2002, Edinburgh (to be published).

19) R. G. Mani, J. H. Smet, K. von Klitzing, V. Narayanamurti, W. B. Johnson, and V. Umansky, *Nature* 420, 646 (2002).

20) M. A. Zudov, R. R. Du, R. R. Simmons, and J. L. Reno, *Phys. Rev. B.* 64, 201311 (2001).

21) M. A. Zudov, R. R. Du, L. N. Pfeiffer and K. W. West, *Phys. Rev. Lett.* 90, 046807 (2003).

22) J. C. Phillips, preprint cond-mat/0212416; A. C. Durst, S. Sachdev, N. Read, and S. M. Girvin, preprint cond-mat/0301569; A. V. Andreev, I. L. Aleiner, and A. J. Millis, preprint cond-mat/0302063; P. W. Anderson and W. F. Brinkman, preprint cond-mat/0302129; K. N. Shrivastava, preprint cond-mat/0302320; J. Shi and X. C. Xie, preprint cond-mat/0302393; A. A. Koulakov and M. E. Raikh, preprint cond-mat/0302465.

23) V. I. Ryzhii, *Sov. Phys. - Sol. St.* 11, 2078 (1970).

24) G. E. Stillman, C. M. Wolfe, and J. O. Dimmock, *Sol. St. Comm.* 7, 921 (1969).

25) The exponential damping of the radiation induced resistance oscillations could be rewritten in a Dingle form, $\exp(-\lambda/B) = \exp(-\pi/\omega_c\tau_f) \approx \exp(-T_f/B)$, where T_f and τ_f represent a finite frequency broadening-temperature and lifetime, respectively. In this interpretation, $\lambda = 65$ mTesla (Fig. 4(a)(iii)) corresponds to $T_f = 64$ mK. See also T. Ando, A. B. Fowler, and F. Stern, *Rev. Mod. Phys.* 54, 437 (1982).